Original Research Article

Effect of gamma radiation in undoped SnO_2 thin films

Abstract.

This paper was reported on study the effect of gamma radiation on nanoporous SnO_2 electrodes for dye-sensitized solar cells. Structural, optical and electrical properties were studied. The refractive index was decreased with the increase in gamma radiation. The resistivity of thin films was decreased about 40% with the increase of gamma radiation at 659 nm film thicknesses. The mobility and carrier concentration were increased with the increase of gamma dose at 659 nm film thickness.

Key words: $SnO_{2;}$ semiconductors; optical; electrical and radiation

1. Introduction

Tin oxide has attracted great attention and many uses in recent decades because of its high transparency and conductivity combined with superior stability. The major applications of transparent conducting oxides include thin-film photovoltaic [Stefik et al, 2013], gas sensors [Huang et al 2006, Yang et al 2006, Simakov et al 2006 and Jin et al 2006], optoelectronics [Wang et al 2005], heat reflectors in solar cells windows [Maghanga et al 2011]. The above-mentioned properties make them very useful in many fields of applications: transparent electrodes for silicon and SeTe and GeSeTe alloys [Maged et al 2010]. The ionizing radiation is available especially as gamma, and determination of its effect is important for the efficient usage of devices on the satellites, space shuttles and industrial Cobalt units [Bhata et al 2007]. Glass materials are broadly used in the application areas of low-orbit satellites and spacecrafts [Maged et al 1998]. Therefore, examination of radiation effects on the glass materials is imperative as well. These effects are associated with the energy of radiation, as well as the total dose [Goswami, 2003].

2. Experimental procedure

2.1 Spray pyrolysis was a chemical deposition technique where the endothermic thermal decomposition was taken place at the hot surface of the substrate to give the final product. The nano-structured films were prepared from crystalline hydrate of tin tetrachloride ($SnCl_4.5H_2O$) which had weight of 5gm by dissolution in 5mL pure methanol. The substrate temperature was in the range of 400–500°C. After the deposition, the films were dried for 1 hour at room temperature. The film thickness was estimated from UV-Vis spectrophotometer, and found 191, 232, 478 and 659 nm, respectively. The deposited thin films were confirmed by X-ray diffraction

examination using an X-ray diffractometer Shimadzu machine model (XD-DI series) with Cu-Kα radiation as a target, λ=1.548 Å, operated at 400 kV and 30 mA using Bragg–Brentano method. The average crystallite size was estimated from the width of x-ray lines by Scherrer's method. The optical transmittance spectra of SnO_2 films were measured in the wavelength range from 190 to 1100 nm by means of the Specord 210 plus UV-Vis spectrophotometer. The electrical properties were studied by sheet resistance method by using RCL meter at room temperature (The Philips / Fluke PM6303A RCL Meter). All measurements were made using a 4-wire technique, which ensures high-accuracy measurements, even for low-impedance components. SnO_2 films were exposed to a Co-60 gamma-radiation source with a dose rate 2.32 kGy. hr^{-1} at room temperature in National Center for Radiation Research and Technology, Egyptian Atomic Energy Authority. The selection of exposure dose was in the range 0.5-22 kGy which is based on industrial applications.

3- Result and discussion

3-1 X-ray analysis

It was seen that the pattern of the SnO_2 film with diffraction peaks at about positions 26.8, 35.3, 37.4, and 52.4 degree, correspond to diffraction signals produced by the (110), (101), (200) and (211) crystalline planes of the tetragonal structure of Tin element. These peaks were increased with the increase of thickness at same positions. It was observed that no change in the peak intensity and position after gamma radiation up to 22 kGy (data not shown). Assuming a homogeneous strain across crystallites, the crystallite size of nano-crystallite was calculated from the full width half maximum (FWHM) values by using the Scherrer formula for crystallite size broadening of diffraction peaks,

$$\boldsymbol{D = \frac{0.9\,\lambda}{B\cos\theta}} \qquad (1)$$

where D is crystallite size, λ is the wavelength of x-ray, B is FWHM of diffraction peak and θ is the diffraction angle. The crystallite size of tin oxide thin film thickness of 191, 232, 478 and 659 nm were found to be 8, 8, 9 and 16.

3-2 Theoretical background of optical transition

Basically, there are two types of optical transition that can occur at the fundamental edge of crystalline semiconductors: direct and indirect transitions. For simple parabolic bands ($N(E) \alpha E^{1/2}$) and for direct transitions,

$$\alpha(\nu)n_o h\nu \approx (h\nu - E_g)^n \qquad (2)$$

Where, α is the absorption coefficient, n is a constant of ½ for allowed transitions and of 3/2 for forbidden transitions in the quantum-mechanical sense, n_o is the refractive index which is assumed to be a constant over energy variation, $h\nu$ is photon energy and E_g is the band gap energy of the material under investigation. This type of absorption is independent of temperature apart from any variation in E_g.

3-3 Optical absorption shift:

There is α shift in the band gap towards higher energy for the thin film having higher carrier density. This shift was due to the filling of the states near the bottom of the conduction band [Burstein, 1954 and Moss, 1954]. The shift was given by the relation.

$$E_g = E_{go} + \Delta E_g^{BM} \qquad (3)$$

where $\mathbf{E_{go}}$ is the intrinsic band gap and $\mathbf{\Delta E_g^{BM}}$ is **the** BM shift. The shift is related to the carrier density as

$$\Delta E_g^{BM} = \frac{\pi^2 h^2}{2m^*} \left(\frac{3N}{\pi}\right)^{2/3} \qquad (4)$$

where m* is the reduced effective mass and N is carrier density.

3-4 Optical band gap

The direct transition property of SnO_2 films, Eq.2 was applied with n =1/2 in the case of the crystalline film, and with n = 2 which could be applied to amorphous film [Maged et al 2010**]**. The optical properties mainly depend on the refractive index of the material and thickness of the film. The absorption and dispersion of a plane electromagnetic wave was described by the complex refractive index $\grave{N} = n + ik$, where n is the real refractive index and k is the extinction coefficient. The physical significance of k is that on traversing a distance in the medium equal to one vacuum wavelength, the amplitude of the wave decreases by the factor $\exp(-2\pi ik)$. It was observed that the decrease in the transmission with the increase in thin film thicknesses at different wavelength for tin oxide thin film (data not shown). The transmission spectra of glass substrate and as deposited before and after gamma radiation were shown in Fig. 1.

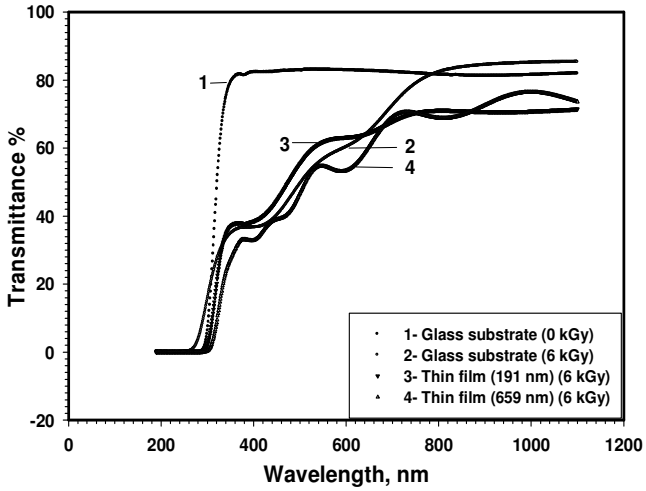

Fig. 1. Transmission spectra of glass substrate and as deposited films before and after gamma radiation.

It was noticed that a decrease 63% in transmission for the glass substrate after gamma radiation exposure. This decrease might be due to that the transparent glass was converted into brown color after exposing to 6 kGy gamma dose. There was absorption coefficient, α shift at absorption edge towards higher energy with the increase of film thicknesses (data not shown).

The absorption coefficient difference (δ) as a function of gamma dose for SnO_2 at 191 nm film thickness was shown in Fig.2. There was an exponentially increase up to gamma dose 6 kGy, and so, it could be possible to use as gamma dosimeter up to 6 kGy which is used in the industrial applications. The same thing was taken placed to the extinction coefficient.

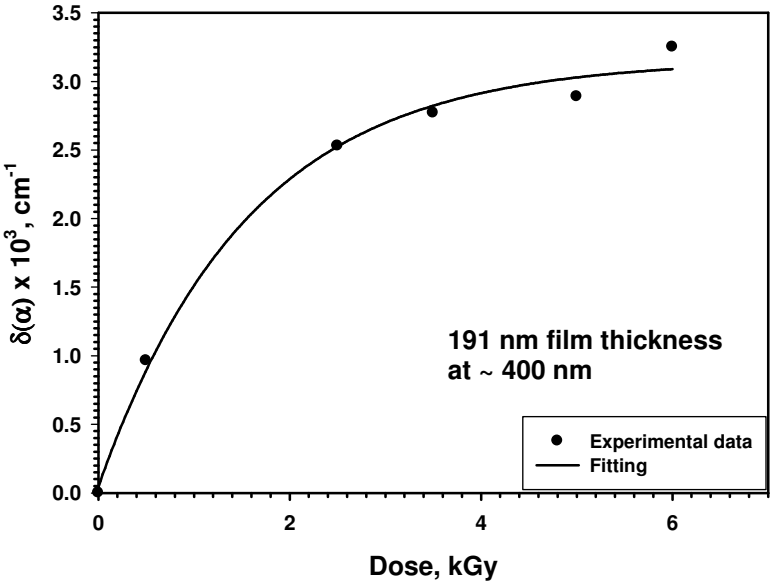

Fig. 2 Absorption coefficient difference (δ) as a function of gamma dose of selected film..

The absorption coefficient, α, as a function of wavelength for SnO_2 at 659 nm film thickness in the interference area was shown in Fig.3. There was an increase in the absorption coefficient with the increase in wavelength and more increase after gamma radiation. The absorbance as a function of wavelength in the interference area before radiation (Fig.3-1) has different orientation behavior from the radiated sample (Fig.3-2). The same behavior of (α) was observed to the extinction coefficient (k).

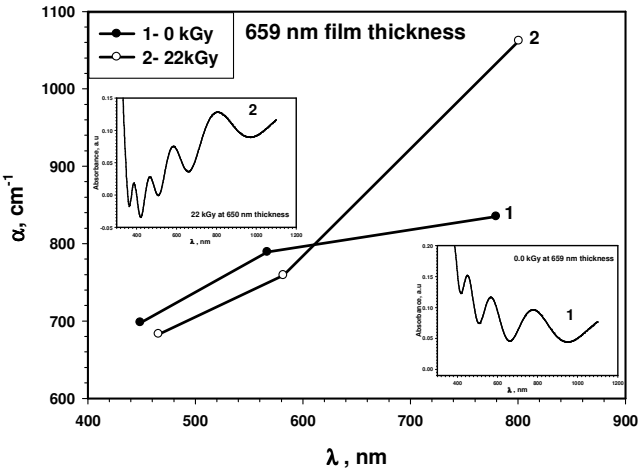

Fig. 3 The absorption coefficient, α vs. wavelength in the interference area of film before and after radiation.

The refractive index was decreased with the increase of wavelength before and after radiation as shown in Fig. 4. The refractive index and extinction coefficient for the thin film at thickness range 191-659 nm were calculated in the interference area. The refractive index in this study was coincidence with atomic layer deposition method of tin oxide films [Elam, 2008]. The absorbance as a function of wavelength before and after radiation was shown in Fig. 4(1&2).

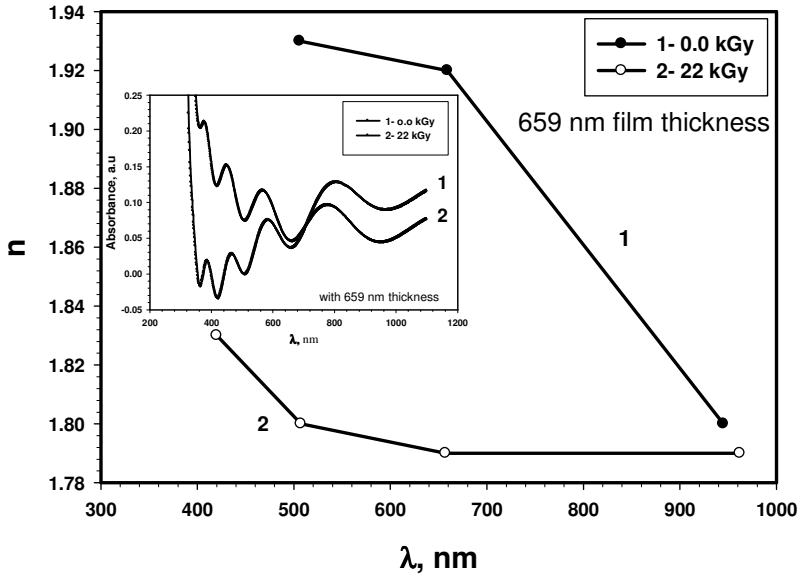

Fig. 4 The refractive index vs. wavelength in interference area of film before and after radiation.

Our results were relatively matching the changes in the refractive index correspond to the fact that the refractive indices of SnO_2 were 1.96 and 1.79 before and after gamma radiation, respectively [Elam et al 2008, Heo et al 2010]. At wavelength range 400–950 nm (1.3–3.1 eV), the values of k were in the range of 1.6 x10^{-2} –1.8 x 10^{-2} before radiation and it was found in the range 0.3x 10^{-2} - 3.2 x10^{-2} after radiation. As reported in [Habibi and Talebian 2005] the refractive index of SnO_2 at 550 nm is 2.0 and the extinction coefficient was 0.03 and these results were relatively consistent to this work. The high absorption coefficient was observed for the SnO_2 films due to the polycrystalline of the sample, which was evident from the x-ray studies.

The direct band gap of tin oxide were reported 4.3 eV [Spence 1967], 3.1 eV [Reddy and Chandorkar 1999] and 3.95 eV [Sundaram and Bhagavat, 1981]. In the present

report, the direct band gap obtained was 3.88 eV at an atmospheric pressure of 1.01 x 10^{-5} Pa and room temperature before radiation and 3.96 after radiation. The variation of the direct band gap with radiation for 191 and 659 nm film thicknesses were may be due to the Burstein-Moss shift.

3-5 Electrical properties

It was found that the sheet resistance decreased from 16 kΩ/□ to 3 kΩ/□ with the increase of film thickness. The resistivity was decreased from 32× 10^{-2} Ω-cm, to 12 × 10^{-2} Ω-cm after radiation for 191 nm film thickness. It was found that the resistivity decreased exponentially with the increase gamma dose and it might be used as gamma dosimeter (data not shown). The mobility and carrier concentration were found 1.1 cm^3/V-s and 1.9 × 10^{19}/cm^3, respectively before radiation at 191 nm film thickness. These values were found relatively consistent with the values was reported [Elam et al 2008 and Heo et al 2010]. The mobility and carrier concentration were increased with the increase of radiation at 659 nm film thickness.

Conclusion

The structural, optical and electrical properties of SnO_2 thin films on glass substrates were evaluated before and after gamma radiation. X-ray diffraction was revealed that the SnO_2 films were crystalline. A red shift in the absorption edge was observed with the increase of thickness. The thin film deposited on glass was yielded optical transmission of 94% at 191 nm film thickness. The optical energy gap was increased to 3.95 eV at gamma dose 6 kGy. There was absorption coefficient, α shift in the band gap towards higher energy for the thin film which having higher carrier density. At wavelength range 400–950 nm, the values of extinction coefficient were in the range of 1.6 x10^{-2} -1.8 x 10^{-2} before radiation and it was found in the range 0.3 x 10^{-2} - 3.1 x10^{-2} after radiation. Radiation was induced changes in the optical and electrical properties of SnO_2 films resulted in the degradation of their performance.

References

- Bhata J.S., Maddani K.I. , Karguppikar A.M., Ganesh S. 2007. Nuclear Instruments and Methods in Physics Research B , 258(2), 369–374.

- Burstein E. 1954. Phys. Rev., 93, 632–633.
- Elam W. J., Baker A. D , Hryn J. A., Martinson B. F. A., Pellin J. M., Hupp T. J. 2008. J. Vac. Sci. Technol. A, 26(2) 244–252.
- Goswami A. 2003. Thin Film Fundamentals, New Age International (P) Limited, Publishers, New Delhi.
- Habibi M. H., Talebian N. 2005. *Acta Chim. Solv.* 52, 53.
- Heo J., Hock A. S., and Gordon R. G. 2010. J. Chem. Mater., 22, 4964–4973.
- Huang X. J., Choi Y. K., Yun K. S., and Yoon E. 2006. Sens. Actuators B 115, 357.
- Jin C. J., Yamazaki T., Ito K., Kikuta T., and Nakatani N. 2006. Vacuum 80, 723.
- Maghanga A., Niklasson G. G., Granqvist C., and Mghendi M. 2011. APPLIED OPTICS, 50, 19 /1.
- Maged A.F., Amin G.A.M., Semary M, E. Borham 2010. Thin Solid Films 518, 2628–2631.
- Maged A.F, Montasser K.I. and Amer H.H. 1998. J. Materials Chemistry and Physics, 56/2,184-188.
- Moss T. S. 1954. Proc. Phys. Soc. B, 67, 775–782.
- Reddy M. H. M. and Chandorkar A. N. 1999. Thin Solid Films, 349, 260.
- Simakov V., Yakusheva O., Grebennikov A., and Kisin V. 2006. Sens. Actuators B 116, 221.
- Stefik M, Heiligtag F. J., Niederberger M., and Grätzel M. 2013. *ACS Nano*, 7 (10), 8981–8989.
- Spence W. 1967. J. Appl. Phys, 38, 3767.
- Sundaram K.B. and Bhagavat G.K. 1981. *J.* Phys. D: Appl. Phys., 14, 921.
- Wang G. F., Tao X. M., and Huang H. M. 2005. Color. Technol. 121, 132.
- Yang H. M., Zhang X. C., and Tang A. D. 2006. Nanotechnology 17, 2860.